JOURNAL OF SOLID STATE CHEMISTRY 12, 341–348 (1975)

Non-Steady-State Phenomena in Defect Thin-Film Metal–Insulator–Metal Systems Containing Schottky Barriers*†

J. G. SIMMONS

Electrical Engineering Department, University of Toronto, Toronto, Canada

AND

G. S. NADKARNI

Precision Electronics Components, Toronto, Canada

Received July 3, 1974

The electrical properties of metal–insulator–metal systems are presented. It is shown at low temperatures the capacitance is inversely proportional to insulator thickness, as expected, but at high temperatures the capacitance of such samples is *independent* of insulator thickness.

Depending on the relative magnitudes and polarity of the bias applied during cooling and heating, the dc current–temperature characteristics exhibit pronounced structure. Also, the current may flow either positively (conventionally), negatively (counter conventionally), or in both directions. Steady-state and non-steady-state behavior are distinguished, the former being electrode limited and the latter bulk limited, and it is shown how to extract various system parameters, such as interfacial barrier heights, the bulk activation energy and trap density, from the *I–T* characteristics.

1. Introduction

Conduction processes through insulators are often described in terms of the conventional Schottky or Poole–Frenkel effects. Both these effects are reflected in the current (I) vs voltage (V) characteristics by the relationship.

$$\ln I \propto V^{1/2}. \qquad (1)$$

(Note that the term "conventional" used above also signifies that I above is a steady-state current.) This result is predicated on a conduction band that is flat and undistorted throughout the insulator before and after the voltage is applied. However, it is a fact that if localized states (traps) are distributed throughout an insulator (and this is generally thought to be the case for real insulators, and is definitely the case for amorphous insulators), then the band edges are, in general, severely distorted at the electrode–insulator interface.

Consider the case when the electrode work function ψ_m is greater than that, ψ_i, of the insulator, the traps in which are filled to a level (the Fermi level) E_t below the bottom of the conduction band, as shown in Fig. 1a. Thus, when the electrodes are applied, electrons in traps located below the Fermi level in the insulator are transferred to the electrodes, depleting the higher-energy insulator traps close to the interface. This charge-transfer process increases the potential energy of the electrons in the electrodes with respect to those in the insulator, and ceases when the Fermi levels in the insulator and the electrodes line up, as shown in Fig. 1b. When the trap density is high ($>10^{17}$ cm^3), as in the case of amorphous insulators, the positive space charge is located just—a few hundreds of angstroms or so—inside the surface of the insulator, and causes the band edges of the insulator close to the surface to bend upwards, giving rise to pronounced Schottky (blocking) contacts at the metal–insulator interface (*1–3*).

* Invited paper.

† Work supported by the National Research Council and Defense Research Board of Canada.

Copyright © 1975 by Academic Press, Inc.
All rights of reproduction in any form reserved.
Printed in Great Britain

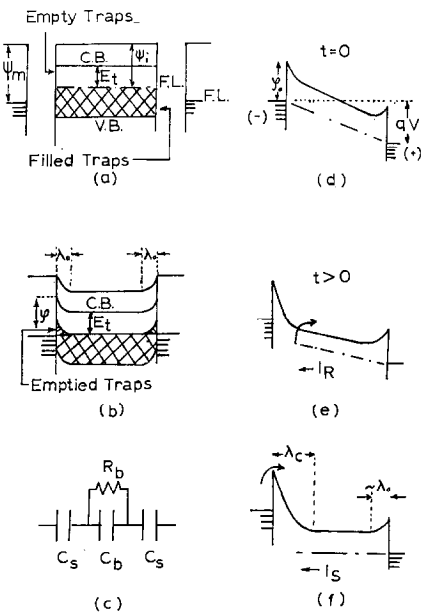

FIG. 1. (a) Energy diagram before electrodes applied to insulator; (b) after electrodes applied; (c) equivalent ac circuit for (b). Diagrams (d)–(e) are energy diagrams for system; (d) immediately after applying voltage bias ($t = 0$); (e) during relaxation; (f) in steady state.

This type of contact gives rise to interesting steady-state and non-steady-state behavior. The steady-state characteristics do not obey the relationship given by Eq. (1), and the non-steady-state behavior has, by and large, been overlooked or ignored or simply not recognized, yet it is this behavior that yields the most information about the system.

With these ideas in mind, let us now look at selected experimental data on Al–CeF_3–Al samples which demonstrate some of the more interesting non-steady-state characteristics associated with insulators containing Schottky barriers.

2. Fabrication

The samples were fabricated on a glass substrate by vacuum deposition of successive layers of aluminum, cerous fluoride (CeF_3), and aluminum. The deposition was made at a pressure less than 10^{-5} Torr. The first electrode (lower electrode) was deposited in the form of a strip $1\frac{3}{4}$ in. long and $\frac{1}{8}$ in. wide. The cerous fluoride was then deposited at a rate of about 8 Å sec^{-1}, and ranged locally, in steps, from 1800 to 4900 Å on the substrate. Finally, the counter electrodes were deposited perpendicular to the lower electrode, in the form of strips $\frac{1}{8}$ in. wide and $\frac{1}{2}$ in. long, so as to produce 12 Al–CeF_3–Al capacitors on the substrate.

3. Alternating Current Measurements

The capacitance vs reciprocal insulator thickness measurements shown in Fig. 2 reveal directly the effect of Schottky barriers. The lower curve, measured at 100°K shows the capacitance to be *inversely proportional* to reciprocal thickness, as expected. In contrast, the upper curve, obtained at 400°K, shows the capacitance to be *independent* of the thickness.

These results can be explained (*4*) on the basis of the equivalent circuit for the sample, shown in Fig. 1c. In this inset C_s represent the capacity of the Schottky barriers, and C_b the capacity of the interior of the insulator, i.e.,

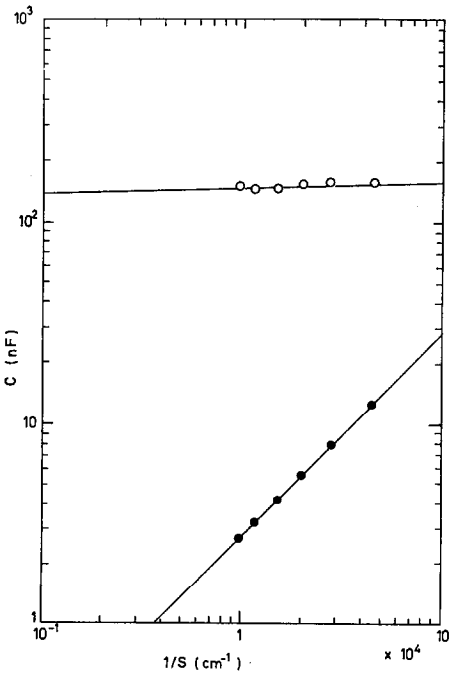

FIG. 2. Capacitance (c) vs inverse thickness. 77°K; ○ 390°K.

the region between the two Schottky barriers, which has a temperature dependent resistance R_b

$$R_b = R_o \exp(E_t/kT)$$

in parallel with it, where R_o is a parameter with units of resistance, E_t is the activation energy of the interior of the insulator and k is Boltzmann's constant. Thus at low temperatures where R_b is very large, essentially infinite as far as we are concerned here, the capacitance is simply the series sum of the capacitance of the two Schottky barriers and the interior, or, in other words, the geometric capacitance which accounts for the linear relationship between capacitance and inverse thickness illustrated by the lower curve. At high temperatures, R_b becomes very small and shunts C_b, which means that the capacitance is equal to the series sum, $C_s/2$, of the two Schottky barriers, which is of course independent of thickness, as observed.

4. Current–Temperature Characteristics

a. Preliminary Comments

Figures 1d–1f illustrate the energy diagrams at various times after a voltage has been applied to the system (*2*). Figure 1d represents the case immediately after application of the voltage, which is shown uniformly distributed throughout the insulator. This is clearly an unstable state, since the cathodic depletion region (CDR) (i.e., the space charge region) being blocking requires to have the majority of the applied voltage across it. Thus, for $t > 0$, Fig. 2e, electrons are excited out of traps at the edge of the CDR resulting in the growth of, and hence an increase in the potential drop across, the CDR. The current associated with this release of electrons is the non-steady-state relaxation current I_R, which has an activation energy $E_t(= E_c - E_f)$, i.e., $I_R \propto e^{-E_t/kT}$, and is much greater than that flowing over the cathodic barrier, which has an activation energy $\phi > E_t$, i.e., $I \propto e^{-\phi/kT}$. The relaxation process and, hence, I_R cease when the sample reaches the steady state.

Figure 2f represents the energy diagram for the steady state, in which most of the voltage is dropped across the CDR and only a small portion across the interior and the anode depletion region (ADR), just sufficient to maintain current continuity throughout the system. In the steady state, the current is the steady-state Schottky–Richardson I_s that flows over the cathodic barriers. This current is thickness independent, and determined by the height of the cathodic barrier (*3*), that is

$$I_s = AT^2 e^{-\phi/kT} \text{ A/cm}^2 \qquad (2)$$

where $A = 120$ Å/cm^2 K^2, k is Boltzmann's constant and T is the temperature (°K).

At low temperature the non-steady state depicted by Fig. 1d will prevail indefinitely since the rate of release of electrons, and hence I_R will be very small. On the other hand, at high temperatures where the rate of emission is high, the system will relax rapidly to the steady state (Fig. 4f).

b. Steady-State I–T *Measurements*

Prior to cooling, the voltage has to be applied at a high temperature for 30 min, to ensure the sample has had time to relax to the steady state.

The curves shown in Fig. 3 were obtained with the same bias voltage applied during cooling (V_d) and heating (V_i), that is, $V_d = V_i$;

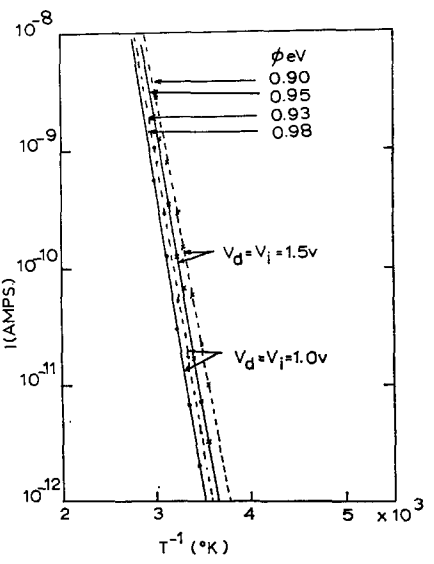

FIG. 3. Steady-state ln I vs T^{-1} characteristics ($V_i > V_d$).

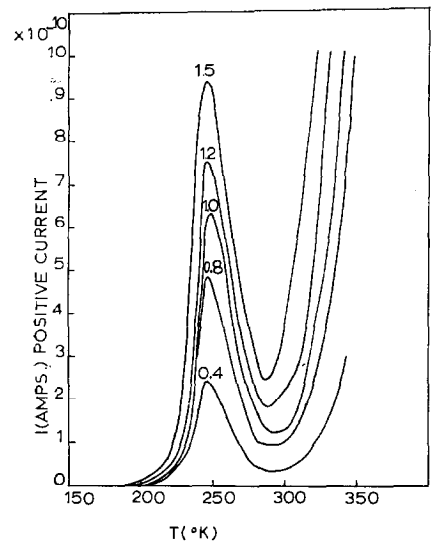

FIG. 4. Non-steady-state I vs T characteristic. $V_d = 0$ V.

thus, these curves are the *steady-state* characteristics. The full curves were obtained with the counter electrode positively biased, and the dotted curves with the counter electrode negatively biased. The voltage bias used during the measurements is stated alongside the curves.

The salient features of these curves are: (a) they each have a well-defined (constant) activation energy; (b) the activation energy for a particular voltage bias is greater when the counter electrode is positively biased; and (c) the activation energy of both sets of curves decreases slightly with increasing voltage bias. These characteristics were found to be independent of the rate of increase of temperature, which is, of course, a characteristic property of a steady-state measurement, and independent of the sample thickness, which indicates that the process is electrode limited. Thus, the ϕ values represent the interfacial barrier heights, for the particular applied voltage, the reduction in ϕ with increasing applied voltage being due to image-force lowering of the barrier. Note that the interfacial barrier height at the counterelectrode is smaller than that at the interface of the lower electrode.

b. Non-Steady-State Characteristics

i. $V_d = 0$, $V_i > 0$. Figure 4 illustrates non-steady-state I–T characteristics that result when the temperature sample is raised at a rate $B = 0.1$°K/sec. In all these cases the electrodes were *short circuited* during cooling ($V_d = 0$), but heated with different constant V_i (0.4–1.5 V) applied. All the curves are seen to exhibit a single maximum at a temperature $T_m \simeq 250$°K. The magnitude of the maximum current is seen to be greater the greater V_i, and the half width of all the peaks is approximately 30°K. Above about 290°K the current increases monotonically with increasing temperature.

The curve corresponding to $V_i = 1.5$ V in Fig. 4 is shown replotted in the form $\log I$ vs T^{-1} in Fig. 5. At temperatures below T_m this curve has a well-defined activation energy of magnitude 0.68 eV. Above about 300°K the curve again manifests a well-defined activation energy, but in this case its magnitude is 0.95 eV. The chain-dotted line shown in Fig. 5 was obtained under identical experimental

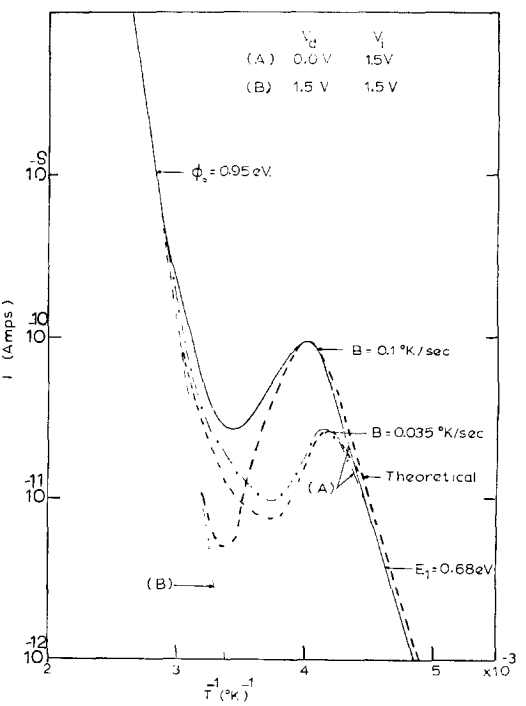

FIG. 5. Non-steady-state ln I vs T^{-1} characteristic for $V =$ characteristic in Fig. 4.

conditions as was the full line except that the heating rate ($B = 0.035°K/sec$) was lower. In this case the magnitude of current and the temperature at which the current maximum occurs are shifted to lower levels, but the two activation energies associated with the two curves are identical. Furthermore, the high-temperature portion of the two curves actually merge, showing that in this range the characteristics are *independent* of the heating rate. The dotted curve shown in Fig. 5 is the *steady-state* characteristic for $V_i = 1.5$ V (see Fig. 3); this curve is seen to have essentially the same activation energy as that portion of the curves in Fig. 5 with which it merges. All the curves shown in Fig. 4 exhibit the same characteristic behavior as that shown in Fig. 5.

Repeating the above experiments but with the voltage polarity of V_i reversed (i.e., with the counter electrode negatively biased) resulted in essentially identical *I–T* characteristics as those described above.

These results may be explained (*5*) with the aid of Figs. 1d–1f. At very low temperatures when the bias is applied, the electrons escape only very slowly from their traps, and the current as a function of temperature is given by

$$I_R = qN_t e_n e^{-e_n kT^2/BE_t}, \tag{3}$$

where

$$e_n = \nu e^{-E_t/kT} \tag{4}$$

and ν is the attempt-to-escape frequency and N_t is the trap density. At low temperatures, Eq. (3) reduces to

$$I_R = qN_d \nu e^{-E_t/kT}, \tag{5}$$

so I_R increases exponentially with T^{-1}, with an activation energy, E_t. Hence, from the linear portion of the low temperature (non-steady-state) portion of the $\ln I$–T^{-1} characteristic we find the activation energy of the interior to be $E_t = 0.68$ eV.

Eventually, as the sample approaches the steady-state, the current falls to its steady-state electrode-limited value, resulting in a peak in the *I–T* characteristic. Thereafter, the (steady-state) current increases with an activation energy of ϕ, the cathodic interfacial barrier height.

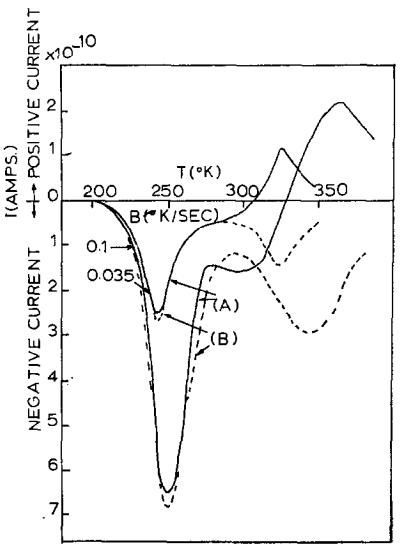

FIG. 6. Non-steady-state I vs T characteristics ($V_i < V_d$). Dotted and full lines correspond to counter-electrode positively and negatively biased, respectively.

The dotted line in Fig. 5 is the theoretical *I–T* characteristic given by $I = I_R + I_s$ (see Eqs. (1) and (2)), using $\phi = 0.95$ eV, $E_t = 0.68$ eV and $N_t = 5 \times 10^{19}$ cm^{-3}, and it is noted the correlation between theory and experiment is extremely good.

ii. $V_d > 0$, $V_i = 0.1$ *V.* The solid curve in Fig. 6 was obtained with the sample heated with $V_i = 0.1$ applied to the counter electrode after the device had been cooled under *steady-state* conditions with a voltage $V_d = 1.0$ V applied to the counter electrode. The dotted curves correspond to identical experimental conditions except that the polarity of bias was reversed.

The interesting feature of the dotted curves is that the current is always *negative*, that is, *if flows the cathode to anode*, i.e., electrons flow from anode to cathode. In the case of the full curve, the lower-temperature portion of the curve is *negative*, but at higher temperatures it becomes *positive*; that is, it flows in the conventional direction, from anode to cathode. Also, both curves exhibit two distinct maxima, in contrast to the single maxima observed in the characteristic in Fig. 4.

These results may be readily explained (*6*) in the aid of the energy diagrams in Fig. 7.

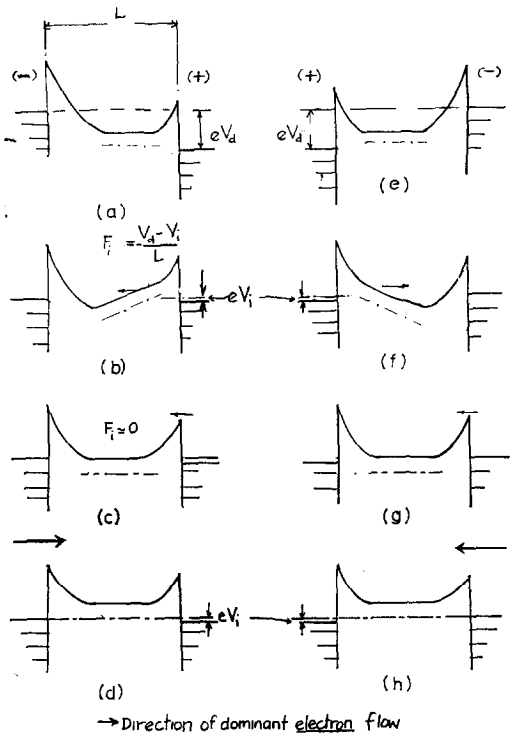

FIG. 7. Energy diagrams for characteristics shown in Fig. 6: (a) in steady state with $V_d(>V_t)$ applied, (b) at low temperature with V_t applied, just prior to heating, (c) in quasi steady state, and (d) in steady state. Diagrams (e)–(h) correspond to (a)–(d), but with polarity of bias reversed. The signs (+) and (−) correspond to polarity of bias.

Figures 7a and 7e represent the sample being cooled in the steady state with $V_d = 1.0$ V applied with the counter electrode positive and negative, respectively. Figures 7b and 7f correspond to the sample at very low temperature with the voltage reduced to $V_t = 0.1$ V. At very low temperatures the sample cannot relax to the steady state so the effect of reducing the voltage induces an electric field, F_t, of strength $(V_d - V_t)/L$ in the interior of the insulator, where L is the insulator thickness, such as to drive *electrons* from the anode to the cathode.

To understand the origin of the lower-temperature peak let us assume that in applying the initial steady-state voltage V_d, the charge in the cathodic depletion increased by an amount, Q_d. Now since $V_t = 0.1 \simeq 0$ V, then if the device is to reach the steady-state approximately Q_d of negative charge has to be supplied to the CDR in order to reduce its charge to approximately its zero-bias value. Assuming that the anodic barrier is blocking, then this charge has to be supplied by electrons being excited out of the edge of the ADR. Hence, as the temperature increases, the rate of release of electrons from traps and, hence, the non-steady-state current initially increases. These electrons are driven away from the anode towards the CDR by virtue of the direction of the field in the interior of the insulator, thus giving rise to a negative current. Clearly, the ADR grows while the CDR decreases, with a corresponding reduction in the field in the interior of the insulator. The non-steady-state current begins to drop when the field in the interior approaches zero; since $V_t \simeq 0$ (Figs. 7c and 7g), this obviously occurs when the width of the ADR equals that of the CDR, i.e., when the voltage drop in both barrier regions are approximately equal. In this case both the CDR and the ADR contain an excess positive charge of approximately $Q_d/2$, the ADR having supplied a negative charge $-Q_d/2$ to the CDR. The fact that both depletion regions contain excess positive charge over and above their zero-bias value means that the device is not in the steady state, but rather a quasi steady state.

The higher-temperature peak in Fig. 6 is associated with the relaxation of the system from the quasi steady state to the steady state (Figs. 7d and 7h). In this case electrons are injected from the electrodes into the insulator. If the barrier height at the two interfaces were identical, then the two currents at the contacts associated with this process would be equal and opposite, and there would be zero current flow in the external circuit. However, we deduced from the experimental results in Fig. 3 that the barrier height at the counter electrode is smaller than that at the lower electrode. Hence, in relaxing to the steady state a greater neutralizing *electron* current flows across the counterelectrode interface, as indicated by the arrow in Figs. 7c and 7g. Thus, for the case when the counterelectrode is positively biased, it will be apparent from Figs. 7b and 7c that this current flows in the

same (negative) direction as that associated with the low-temperature peak, as is observed experimentally. However, for the case when the counterelectrode is positively biased, it is apparent from Figs. 7f and 7g that this current flow is in the opposite (positive) direction to that of the lower-temperature peak. Of course, this current initially increases with increasing temperature; however, as the excess positive charge in the insulator approaches zero the nonsteady current approaches zero, resulting in the observed second peak at higher temperatures in the *I–T* characteristics. Thereafter, the current that flows in the system is the (low) steady-state current associated with the Schottky–Richardson current over the cathodic (negatively biased electrode) interface, which, of course, flows in the positive direction.

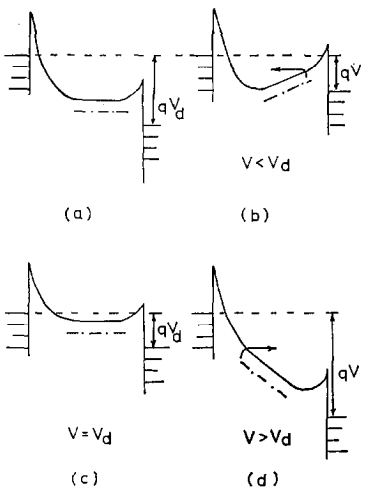

FIG. 9. Energy diagram for characteristics shown in Fig. 8. (a) During cooling; (b) $V < V_d$; (c) $V > V_d$.

5. Non-Steady-State-Isothermal *I–V* Characteristics

Non-steady-state *I–V* measurements were made by applying a voltage V_d at high temperature so that the sample relaxed quickly to the steady state. The sample was then cooled to a predetermined constant low temperature T_0 with V_d still applied, and at that temperature the *I–V* characteristics were generated. The results of this procedure are shown in Figure 8, which illustrates the non-steady-state *I–V* characteristics for several values of V_d and $T_0 = 225°K$. The interesting features of the characteristics are: (a) the *I–V* characteristics are not uniquely defined but *depend* upon V_d, the initial voltage; (b) for $V < V_d$ a negative current flows in the sample, i.e., the direction of the current flow is in the *opposite* direction to the conventional current flow; (c) the current is *zero* for $V \simeq V_d$ and the *I–V* curves for various V_d are essentially parallel; (d) for $V > V_d$ the current flows in the positive direction.

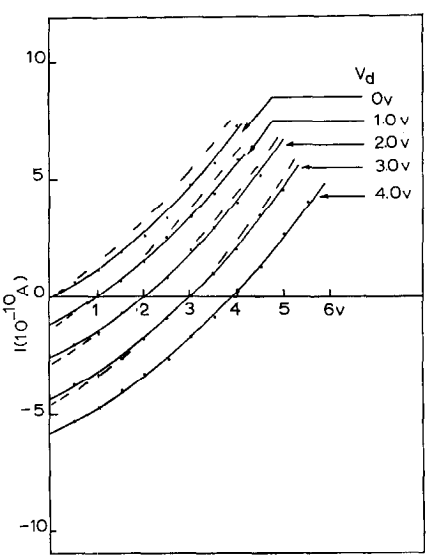

FIG. 8. Isothermal non-steady-state *I–V* characteristics. $T = 225°K$.

These results can be readily explained on the basis that Schottky barriers and non-steady-state conditions exist in the sample, as follows. On the application of the voltage at high temperature, the system relaxes to the steady state as shown in Fig. 9a. Now, provided the voltage is held constant during cooling, the system will be in the steady state at low temperatures. If, however, the voltage is deviated from V_d (Fig. 9b, and 9c) at this temperature, a non-steady-state current flow will be induced in the system. Provided that the temperature is sufficiently low, then the non-steady-state current will be essentially constant in time; *thus an I–V characteristic measured at low temperatures, although apparently steady state is, in fact, non-steady-state*

in nature. For $V < V_d$, the energy diagram under non-steady-state condition will be as shown in Fig. 9b. In this case, it will be noted that the field in the interior, which is equal to $(V - V_d)/L$, is such as to drive electrons from the anode to the cathode; in other words, reducing the voltage below V_d causes *negative* currents to flow, as is observed. For $V > V_d$, the field in the interior is now such as to drive the electrons from the cathode to the anode; that is, a conventional non-steady-state current flows in the system in this case. Because the non-steady-state currents are considerably greater than the steady-state currents, it requires that the voltage only be decreased *slightly* below V_d to induce a negative non-steady-state current capable of neutralizing the conventional current flowing over the cathodic barrier. What this means is that for V just slightly less than $V_d (V \simeq V_d)$, the current in the system is zero, as observed. The above statements are summarized by the following equations [cf. Eq. (5)].

$$I_{\text{SDRC}} = -I_0 \exp[-(E_t - 2\beta F_t^{1/2})/kT], \quad V_d > V \tag{6}$$

$$I_{\text{SDRC}} = I_0 \exp[-(E_t - 2\beta F_t^{1/2})/kT], \quad V_d < V \tag{7}$$

where $F_t = |V_d - V|/L$.

Equations (6) and (7) are shown plotted as dotted curves in Fig. 8, using $E_t = 0.68$ eV, as computed from the experimental results shown in Fig. 4. The correlation is very good and clearly shows the non-steady-state bulk-limited nature of the I–V characteristics, which is to be contrasted with the electrode-limited nature of the steady-state characteristics.

6. Conclusions

We have shown that the electrical properties of metal–insulator–metal system containing Schottky barriers at the metal–insulator interfaces are a strong function of previous voltage history, and exhibit pronounced structure. The structure may be related to *non-steady-state* and *steady-state* process. The characteristics permit a determination of various system parameters, such as trapping density, interfacial barrier heights, and trap depths.

The I–V characteristics at low temperature are shown to be a function of the voltage applied during cooling, indicating that they are non-steady-state in nature.

References

1. J. G. Simmons, *J. Phys. Chem. Solids* **32**, 1987, 2581 (1971).
2. J. G. Simmons and G. W. Taylor, *Phys. Rev. B* **6**, 4793 (1973).
3. J. G. Simmons, *Phys. Rev.* **166**, 912 (1968).
4. J. G. Simmons, G. S. Nadkarni, and M. C. Lancaster, *J. Appl. Phys.* **41**, 538 (1970).
5. J. G. Simmons and G. W. Taylor, *Phys. Rev. B* **6**, 4804 (1973).
6. J. G. Simmons and G. S. Nadkarni, *Phys. Rev.* **B6** 4815 (1973).